Inferring putative transmission clusters with Phydelity

Alvin X. Han[1,2,3]*, Edyth Parker[3,4], Sebastian Maurer-Stroh[1,5] and Colin A. Russell[3]*

[1]Bioinformatics Institute, Agency for Science, Technology and Research (A*STAR), 30 Biopolis Street, Singapore 138671

[2]NUS Graduate School for Integrative Sciences and Engineering, National University of Singapore (NUS), 21 Lower Kent Ridge, Singapore 119077

[3]Laboratory of Applied Evolutionary Biology, Department of Medical Microbiology, Academic Medical Centre, Meibergdreef 9, 1105 AZ Amsterdam-Zuidoost, The Netherlands,

[4]Department of Veterinary Medicine, University of Cambridge, Madingley Rd, Cambridge CB3 0ES, United Kingdom

[5]Department of Biological Sciences, National University of Singapore, 16 Science Drive 4, Singapore 117558

*Corresponding authors: hanxc@bii.a-star.edu.sg or c.a.russell@amsterdamumc.nl

Abstract: Current phylogenetic clustering approaches for identifying pathogen transmission clusters are limited by their dependency on arbitrarily-defined genetic distance thresholds for within-cluster divergence. Incomplete knowledge of a pathogen's underlying dynamics often reduces the choice of distance threshold to an exploratory, ad-hoc exercise that is difficult to standardise across studies. Phydelity is a new tool for the identification of transmission clusters in pathogen phylogenies. It identifies groups of sequences that are more closely-related than the ensemble distribution of the phylogeny under a statistically-principled and phylogeny-informed framework, without the introduction of arbitrary distance thresholds. Relative to other distance threshold-based and model-based methods, Phydelity outputs clusters with higher purity and lower probability of misclassification in simulated phylogenies. Applying Phydelity to empirical datasets of hepatitis B and C virus infections showed that Phydelity identified clusters with better correspondence to individuals that are more likely to be linked by transmission events relative to other widely-used non-parametric phylogenetic clustering methods without the need for parameter calibration. Phydelity is generalisable to any pathogen and can be used to identify putative direct transmission events. Phydelity is freely available at https://github.com/alvinxhan/Phydelity.

Introduction

Recent advances in high-throughput sequencing technologies have led to the widespread use of sequence data in infectious disease epidemiology (Gardy and Loman 2017). In particular, epidemiologically relevant information such as the structure of transmission networks and infection source identification are increasingly inferred from virus phylogenies, especially for measurably evolving viral pathogens like HIV-1 and hepatitis C viruses (Ambrosioni et al. 2012; Bezemer et al. 2015; Matsuo et al. 2017; de Oliveira et al. 2017; Charre et al. 2018). Non-parametric phylogenetic-based clustering tools operate on the assumption that pathogens in a transmission cluster are linked by transmission events rapid enough that molecular evolution between the transmitted pathogens is minimal, and thus genetically more similar amongst themselves than to the ensemble of input isolates (Prosperi et al. 2011; Ragonnet-Cronin et al. 2013). This assumption is generally valid for rapidly evolving pathogens such as RNA viruses as genetic changes between sequences sampled from transmission pairs are generally low (Campbell et al. 2018).

Non-parametric phylogenetic clustering methods typically measure the genetic divergence of sequence pairs either by their genetic distances that are computed from the sequence data directly (Aldous et al. 2012; Ragonnet-Cronin et al. 2013) or by their patristic distances from the inferred phylogenetic tree (i.e. the sum of the inferred phylogenetic branch lengths linking the two sequences; Brenner et al. 2007; Prosperi et al. 2011). The divergence of a cluster can be defined as the median (Prosperi et al. 2011) or largest (Ragonnet-Cronin et al. 2013) pairwise distance between member sequences of the cluster. To define transmission clusters, an upper divergence threshold is implemented either as an absolute distance limit (Ragonnet-Cronin et al. 2013) or as a percentile of the distribution of pairwise sequence distances (Prosperi et al. 2011). A fundamental limitation of these non-parametric phylogenetic clustering tools is the need to define this arbitrary absolute transmission cluster divergence thresholds (termed as ‘cutpoints’ by Villandre et al., 2016). The lack of a consensus definition of a phylogenetic transmission cluster (Grabowski and Redd 2014) coupled with incomplete knowledge of a pathogen’s underlying epidemiological dynamics often reduces the choice of cutpoints to an *ad hoc* exploratory exercise resulting in subjective cluster definitions.

Phydelity is a novel phylogenetic clustering tool designed to negate the need for arbitrarily defined cluster divergence thresholds. Requiring only the phylogenetic tree as input, Phydelity infers putative transmission clusters through the identification of groups of sequences that are more closely-related to one another than the ensemble distribution under a statistically-principled framework. Phydelity, like another phylogenetic clustering tool that we recently developed, PhyCLIP, is based on integer linear programming (ILP) optimisation (Han et al. 2019). However, the two clustering tools are substantially different in their approaches and ILP models such that their clustering results have entirely distinct interpretations. PhyCLIP uses the divergence information of the entire phylogenetic tree to inclusively assign statistically-supported cluster membership to as many sequences in the tree as possible that putatively capture variant ecological, evolutionary or epidemiological processes. To this end, PhyCLIP is useful for sub-species nomenclature development. Phydelity, on the other hand, exclusively distinguishes closely-related pathogens with pairwise sequence divergence that are significantly more likely to be drawn from the same low divergence distribution than that of the ensemble. As such, while PhyCLIP's designated clusters are underpowered to be interpreted as sequences linked by transmission events, clusters inferred by Phydelity can be interpreted as putative transmission clusters (see Supplementary Materials).

To demonstrate the utility of Phydelity in identifying putative transmission clusters, the algorithm underlying Phydelity is first presented in detail. The clustering tool is then applied to both simulated and empirical datasets, including outbreaks of Hepatitis B and C viruses as well as seasonal A/H3N2 influenza virus infections, and compared against results generated by existing phylogenetic clustering methods. Phydelity is freely available at http://github.com/alvinxhan/Phydelity.

Method

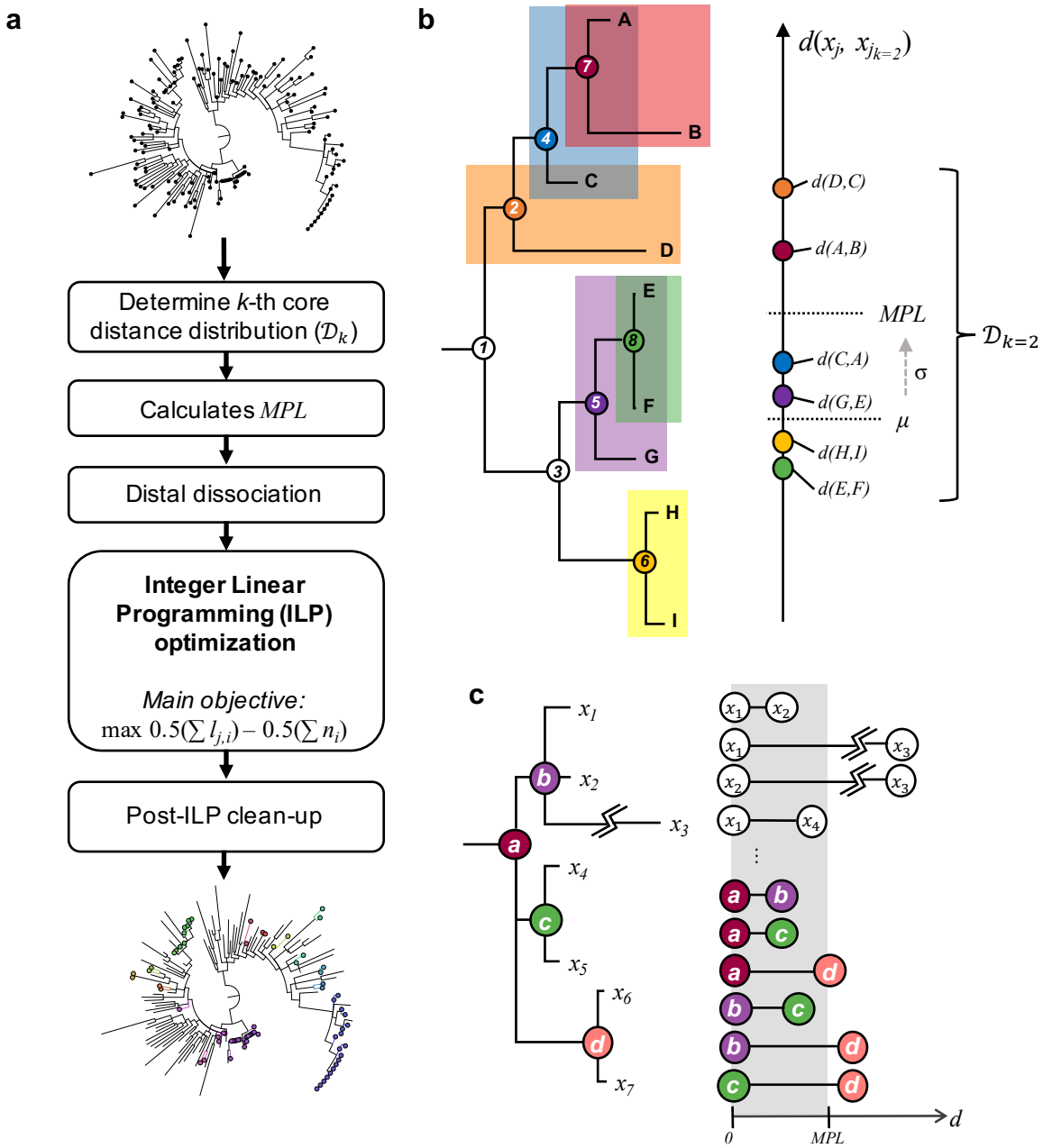

Figure 1. **(a)** Phydelity algorithm pipeline. Phydelity considers the input phylogenetic tree as a collection of putative clusters each defined by an internal node *i* and tips *j* that it subtends. The algorithm first infers the *k*-th core distance distribution ($\mathcal{D}_k$) from the pairwise patristic distances of the closest *k*-neighbouring tips. *k* can be defined by the user or scaled by Phydelity to obtain the supremum $\mathcal{D}_k$ with the lowest divergence. $\mathcal{D}_k$ is then used to compute the maximal patristic distance limit (*MPL*) under which tips are considered to be more closely-related than to the ensemble. Dissociation of distally related subtrees/sequences (Figure 1c) ensues such that both monophyletic and paraphyletic clustering structures can be identified. Phydelity then incorporates the distance and topological information of the remaining nodes and tips into an integer linear programming (ILP) model to be optimised by clustering all tips that satisfy the relatedness constraints within the least number of clusters. Finally, post-ILP steps are implemented to remove any tips that may have been spuriously clustered. **(b)** Determination of the maximal patristic distance limit (*MPL*) using the median (μ) and robust estimator of scale (σ) based on the *k*-th core distance distribution ($\mathcal{D}_k$) of every sequence x_j and its *k*-closest neighbours ($d(x_j, x_{j_k})$; *k*=2 in this case as shown by the pairs of sequences highlighted with distinct colours). **(c)** Distal

dissociation of a putative transmission cluster subtended by internal node ***a***. If a sequence tip has a pairwise sequence distance that is greater than *MPL*, it will be dissociated and not be clustered under the internal node of interest (i.e. internal node ***a***). In this case, sequence x_3 is dissociated from the putative cluster ***a*** due to its exceedingly long branch length violating the *MPL* threshold (i.e. $d(x_3, x_{3_k}) > MPL$). Additionally, whole subtrees subtended by the internal node of interest will be dissociated if any of its inter-nodal patristic distance exceeds *MPL*. Here, subtree ***d*** and its descending sequences (i.e. x_6 and x_7) will be dissociated from ***a*** as its inter-nodal distances with internal nodes ***b*** and ***c*** are both larger than *MPL*.

Clustering Algorithm

Figure 1(a) shows the overall workflow of Phydelity. First, Phydelity considers the input phylogeny as an ensemble of putative clusters, each consisting of an internal node *i* and the leaves it subtends. The within-cluster diversity of node *i* is measured by its mean pairwise patristic distance (μ_i). The patristic distance between two nodes, which can be any sequence tips or internal nodes in the phylogeny, refers to the sum of branch lengths linking those two nodes. Sequences subtended by *i* (i.e. all descendant tree tips of node *i*) are considered for clustering if μ_i is less than the maximal patristic distance limit (*MPL*), under which sequences are considered more closely-related to one another than the ensemble distribution (Figure 1b).

Phydelity computes the *MPL* by first calculating the pairwise patristic distance distribution of closely-related tips comprising the pairwise patristic distances of sequence x_j to the closest *k*-neighbouring tips (i.e. $d(x_j, x_{j_k}) = d_l$) wherein their closest *k*-neighbours include sequence x_j as well (i.e. the *k*-th core distance distribution, $\mathcal{D}_k$; Figure 1b). Additionally, $\mathcal{D}_k$ is incrementally sorted ($d_l \leq d_{l+1}$) and truncated up to d_L if the common log difference between d_L and d_{L+1} is more than zero:

$$\mathcal{D}_k = \left\{ d_1, \dots, d_l, d_{l+1}, \dots, d_L | d_l \leq d_{l+1}, \lg\left(\frac{d_{l+1} - d_l}{d_l}\right) \leq 0 \right\}$$

The user can opt to either input the desired *k* parameter or allow Phydelity to automatically scale *k* to the value that yields the supremum *k*-th core distance distribution with the lowest overall divergence (i.e. the largest possible *k* that still yields the lowest overall divergence between *k*-neighbouring tips). This is done by testing if $\mathcal{D}_{k+1}$ and $\mathcal{D}_k$ are statistically distinct ($p < 0.01$) using the Kuiper's test (see Supplementary Materials). All clustering results of Phydelity presented in this work were generated using the autoscaled value of *k*.

The *MPL* is then calculated by:

$$MPL = \bar{\mu} + \sigma$$

143 where $\bar{\mu}$ is the median pairwise distance of $\mathcal{D}_k$ and σ is the corresponding robust estimator of
144 scale without assuming symmetry about $\bar{\mu}$ using the Qn method (see Supplementary
145 Materials, Rousseeuw and Croux 1993; Figure 1b).
146
147 This is then followed by dissociation of distantly-related descendant subtrees/sequences to all
148 putative nodes for clustering, thereby facilitating identification of both monophyletic as well
149 as nested paraphyletic clusters (Figure 1c; see Supplementary Materials). Phydelity filters
150 outlying tips from putative clusters under the assumption that viruses infecting individuals in
151 a transmission chain coalesce to the same most recent common ancestor (MRCA).
152 Additionally, Phydelity requires any clonal ancestors in between the MRCA and tips of a
153 putative cluster to be as genetically similar to each other as they are to the tips of the cluster.
154 As such, for a putative transmission cluster, the mean pairwise nodal distance between all
155 internal and tip nodes of a cluster must also be $\leq MPL$ (Figure 1c).
156
157 An ILP model is implemented and optimised under the objective to assign cluster
158 membership to sequences satisfying the aforementioned relatedness criteria within the least
159 number of clusters. In other words, Phydelity uses ILP optimisation to search for the
160 clustering configuration that favours the designation of larger clusters of closely-related
161 sequences which are likely linked by transmission events. Any topologically outlying
162 singletons that were spuriously clustered are removed. Finally, it is important to note that a
163 transmission cluster identified by Phydelity should only be interpreted as a fully connected
164 network of likely transmission pairs without implying any underlying transmission
165 directionality. The full algorithm description and mathematical formulation of Phydelity is
166 detailed in the Supplementary Materials.
167
168 *Assessing clustering results of simulated epidemics*
169 Phydelity was evaluated on phylogenetic trees derived from simulated HIV epidemics of a
170 hypothetical men who have sex with men (MSM) sexual contact network (C-type networks in
171 Villandre *et al.*, 2016). The simulated sexual contact network comprised 100 subnetworks
172 (communities) sampled from an empirical distribution obtained from the Swiss HIV Cohort
173 Study. All communities were linked in a chain initially and additional connections between
174 any two communities were generated at a probability of 0.00075. Subjects in the network
175 could either be in the "susceptible", "infected" or "removed" (i.e. individual was diagnosed

176 and sampled) state. Transmission clusters were attributed to sexual contact among individuals
177 belonging to the same community.
178
179 300 epidemics were simulated for four different weights of inter-community transmission
180 rates (w = 25%, 50%, 75% or 100% of the within-community rate). Two infected individuals
181 were randomly introduced in any of the 100 communities. Transmission time along an edge
182 followed an exponential distribution with rates directly proportional to the associated
183 weights. Time until removal was based on a shifted exponential distribution with the shift
184 representing the minimum amount of time required for a virus to be transmitted to susceptible
185 neighbours. The simulation ended once 200 individuals were in the "removed" state.
186
187 These simulated datasets were tested by Villandre *et al.* (2016) to compare the outputs of four
188 "cutpoint-based" phylogenetic clustering methods where the arbitrary distance threshold
189 defining a transmission cluster (i.e. cutpoint) was computed as the: (i) absolute patristic
190 distance threshold between any two tips (Brenner et al. 2007); (ii) standardised number of
191 nucleotide changes (i.e. ClusterPicker, Ragonnet-Cronin *et al.*, 2013); (iii) percentile of the
192 phylogeny's pairwise sequence patristic distance distribution (i.e. PhyloPart, Prosperi *et al.*,
193 2011) and (iv) height of an ultrametric tree obtained using the weighted pair-group method of
194 analysis (WPGMA). For each method, Villandre *et al*. varied the corresponding cutpoint
195 parameter over an equivalent range of thresholds. Comparing the output clusters generated by
196 the four methods at their respective optimal cutpoint by adjusted rand index (see below), it
197 was found that the WPGMA method tended to produce clusters with better correspondence to
198 the underlying sexual contact structure. As such, clustering results from Phydelity were
199 compared to those obtained by Villandre *et al*. using the WPGMA method. Additionally,
200 Phydelity was also compared to the multi-state birth-death (MSBD) method which inferred
201 transmission clusters on the same simulated datasets by detecting significant changes in
202 transmission rates (Barido-Sottani et al. 2018).
203
204 To assess and compare the output clusters from Phydelity and the aforementioned clustering
205 methods that had been tested on these networks previously, several metrics were used to
206 measure how well the clustering results corresponded with the known sexual contact
207 network:

i. Adjusted rand index (*ARI*). ARI measures the accuracy of the clustering results by computing the frequencies of pairs of sequences of the identical (or distinct) subnetwork(s) assigned to the same (or different) cluster(s) (Hubert and Arabie 1985). ARI ranges between -1 (matching between output clusters and community labels is worse than random clustering) and 1 (perfect match between output clusters and ground truth).

ii. Modified Gini index (I_G). Gini impurity, commonly used in decision tree learning, refers to the probability of a randomly selected item from a set of classes being incorrectly labelled if it was randomly labelled by the distribution of occurrences in the class set (Breiman et al. 1984). Here, I_G measures how often a randomly selected sequence from the given network would be incorrectly clustered by the inferred clusters. For a sexual contact network with T communities (i.e. $t \in \{1, 2, \dots, T\}$), I_G is computed as:

$$I_G = \sum_{t=1}^{T} \left[p_t \left(1 - \sum_{c=1}^{C^*} p(c|t) \right) \right]$$

where C^* is the set of clusters defined to have correctly classified sequences attributed to community *t* (i.e. any cluster that constitutes the largest proportion of sequences from community *t* at both the cluster and the community label levels), p_t is the probability of sequence from community *t* and $p(c|t)$ refers to the probability that a sequence is clustered under cluster *c* conditional of it being from community *t*. If output clusters perfectly align with the underlying sexual contact network (i.e. one cluster only constitute one class of community), $I_G = 0$. Conversely, if clustering results are completely random, $I_G = 1$.

iii. Purity measures the average extent that the output clusters contain only a single class (i.e. a particular sexual contact community; Manning et al. 2008):

$$Purity = \sum_{c=1}^{C} \frac{1}{N_c} \left(\frac{\max_t \{N_{c,t}\}}{N_c} \right)$$

where N_c is the size of cluster *c*, $N_{c,t}$ is the number of tips from community *t* clustered under cluster *c* and *C* is the set of all output clusters. Note that purity (as well as I_G) can be inflated if the total number of clusters is large (i.e. if each tip is assigned to a unique cluster, purity = 1 and I_G = 0).

iv. Normalised mutual information (*NMI*) trades off the output clustering quality against the number of clusters (Manning et al. 2008):

$$NMI = \frac{I(T,C)}{[H(T) + H(C)]/2}$$

where *H(T)* and *H(C)* are the respective entropies of the network communities and output clusters, and *I(T,C)* is the mutual information between them. If clustering is random with respect to the network community labels, $I(T,C) = 0$ (i.e. $NMI = 0$). On the other hand, maximum mutual information is achieved (i.e. $I(T,C) = I(T,C)_{max}$) either when the output clusters map the sexual contact network perfectly or all clusters have one member only. Hence, to penalise large cardinalities (i.e. number of members in a cluster) while normalising $I(T,C)$ between 0 and 1, *NMI* is calculated since (a) entropy increases with increasing number of clusters and (b) $[H(T) + H(C)]/2$ is a tight upper bound to $I(T,C)$.

Empirical datasets

Phydelity was also tested on three empirical datasets – acute hepatitis C virus infections among men who have sex with men (Charre et al. 2018), hepatitis B viruses collected from members of the same families (Matsuo et al. 2017) as well as A/H3N2 influenza viruses collected from a community-based cohort of households during the 2014/2015 season (McCrone et al. 2018). All phylogenetic trees were reconstructed using RAxML (v8.2.12) under the GTRGAMMA model (Stamatakis 2014).

Comparisons to ClusterPicker and PhyloPart

ClusterPicker (Ragonnet-Cronin et al. 2013) and PhyloPart (Prosperi et al. 2011), two non-parametric phylogenetic clustering tools that are methodologically comparable to Phydelity, were also applied to the hepatitis C and hepatitis B virus datasets for comparisons. Either clustering tool has been previously applied to multiple studies involving different pathogens (Prosperi et al. 2011; Jacka et al. 2014; Bezemer et al. 2015; Bartlett et al. 2016; Coll et al. 2017; de Oliveira et al. 2017; Charre et al. 2018). Other than the phylogenetic tree, both ClusterPicker and PhyloPart also require users to input an arbitrarily-defined genetic distance threshold (as an absolute distance limit for ClusterPicker and percentile of the global pairwise patristic distance for PhyloPart). As such, a range of distance limits (PhyloPart: 0.5-10th

268 percentile; ClusterPicker: 0.005-0.1 nucleotide/site) were applied to both tools. No bootstrap
269 support threshold were implemented for comparability to Phydelity.
270
271 The lowest optimal threshold for the distance range tested was found by maximisation of the
272 mean silhouette index (*SI)* for both ClusterPicker and PhyloPart. The Silhouette index
273 measures how similar an item is to members of its own cluster as opposed to the nearest
274 neighbouring clusters - i.e. a larger mean silhouette index indicates that items of the same
275 cluster are more closely related amongst themselves than to its neighbours (Rousseeuw,
276 1987). No parameter optimisation was required for Phydelity.
277
278 **Results**
279 *Simulated HIV epidemics*
280 Phydelity was applied to simulated HIV epidemics among men who have sex with men
281 (MSM) belonging to a hypothetical sexual contact network structures where transmission
282 clusters were attributed to transmission by sexual contact among individuals belonging to the
283 same subnetwork (see Methods; Villandre *et al.*, 2016). These simulations were originally
284 used to assess the performance of "cutpoint-based" clustering tools, including ClusterPicker,
285 PhyloPart as well as the weighted pair-group method of analysis (WPGMA) which generally
286 attained the highest adjusted rand-index (ARI) score across all simulations when calibrating
287 their respective cutpoint thresholds against the ground-truth. Phylogenetic trees generated
288 from these simulations were also tested by the multi-state birth death (MSBD) method
289 (Barido-Sottani et al. 2018).
290
291 Clustering results from Phydelity were compared to outputs from the MSBD method and
292 those from the WPGMA method achieving the best ARI scores. The purity, modified Gini
293 index (I_G) and normalised mutual information (*NMI*) measures were also used to provide a
294 more comprehensive assessment of the clustering results (Figure 2, Supplementary Figure 3
295 and Supplementary Table 1; see Methods).
296

a

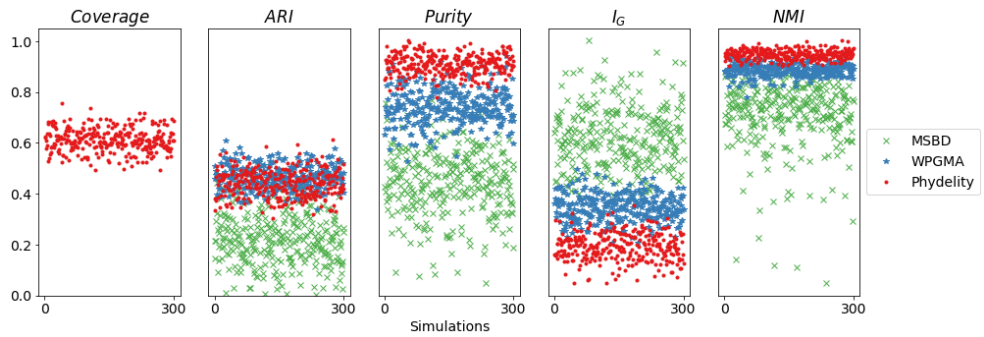
Coverage
ARI
Purity
I_G
NMI
1.0
0.8
0.6
0.4
0.2
0.0
0
300
Simulations
MSBD
WPGMA
Phydelity

b

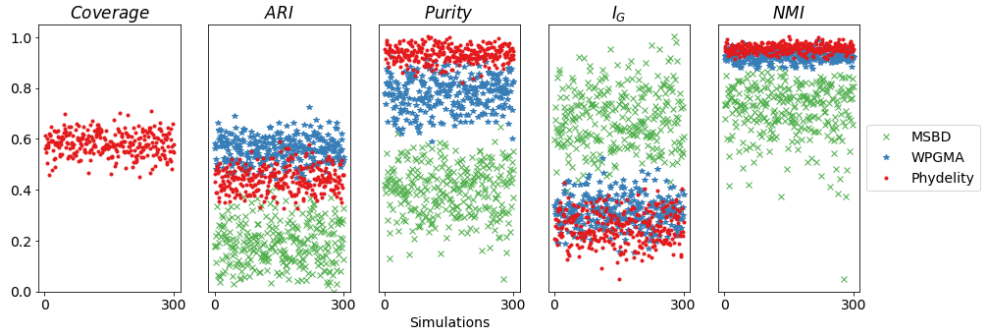
Coverage
ARI
Purity
I_G
NMI
1.0
0.8
0.6
0.4
0.2
0.0
0
300
Simulations
MSBD
WPGMA
Phydelity

c

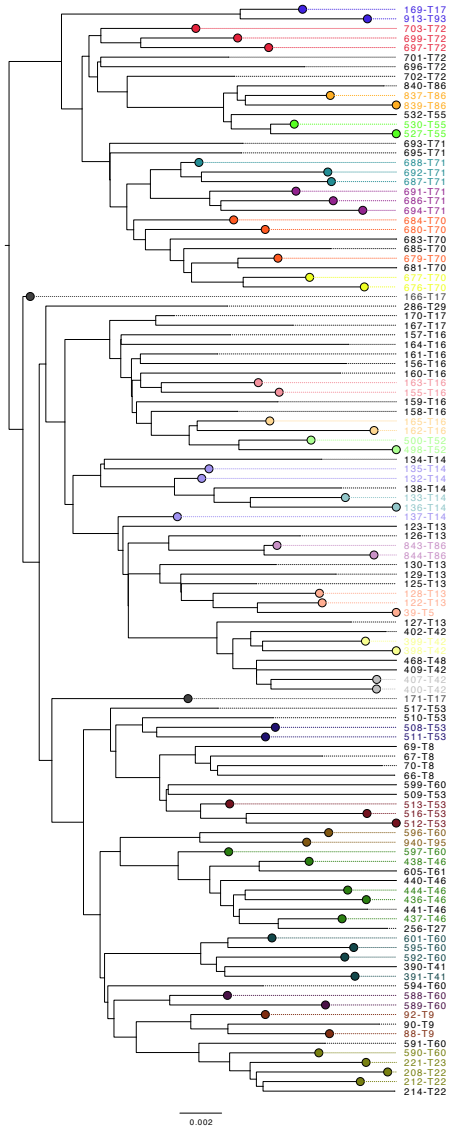
169-T17
913-T93
703-T72
699-T72
697-T72
701-T72
696-T72
702-T72
840-T86
837-T86
839-T86
532-T55
530-T55
527-T55
693-T71
695-T71
688-T71
692-T71
687-T71
691-T71
686-T71
694-T71
684-T70
680-T70
683-T70
685-T70
679-T70
681-T70
677-T70
678-T70
166-T17
286-T29
170-T17
167-T17
157-T16
164-T16
161-T16
156-T16
160-T16
163-T16
155-T16
159-T16
158-T16
165-T16
162-T16
500-T52
498-T52
134-T14
135-T14
132-T14
138-T14
133-T14
136-T14
137-T14
123-T13
126-T13
843-T86
844-T86
130-T13
129-T13
125-T13
128-T13
122-T13
39-T5
127-T13
402-T42
[illegible]
468-T48
409-T42
407-T42
400-T42
171-T17
517-T53
510-T53
508-T53
511-T53
69-T8
67-T8
70-T8
66-T8
599-T60
509-T53
513-T53
516-T53
512-T53
596-T60
940-T95
597-T60
438-T46
605-T61
440-T46
444-T46
436-T46
441-T46
437-T46
256-T27
601-T60
595-T60
592-T60
390-T41
391-T41
594-T60
588-T60
589-T60
92-T9
90-T9
88-T9
591-T60
590-T60
221-T23
208-T22
212-T22
214-T22
0.002

297 **Figure 2**. Clustering results of simulated HIV epidemics in a hypothetical MSM sexual contact network. **(a)**
298 Clustering metrics for clustering algorithms (Phydelity, weighted pair-group method of analysis (WPGMA) and
299 multi-state birth death (MSBD) methods) applied simulated phylogenies with inter-communities transmission
300 rates weighted at half of within-community rates (i.e. $w = 0.5$). Coverage refers to the proportion of tips
301 clustered by Phydelity. Adjusted rand index (*ARI*) measures how accurate the output clusters corresponded with
302 the community labels. *Purity* gives the average extent clusters contain only a single class of community.
303 Modified Gini index (I_G) is the probbility that a randomly selected sequence would be incorrectly clustered.
304 Normalised mutual information (*NMI*) accounts for the trade-off between clustering quality and number of
305 clusters. **(b)** Results for simulations where inter-communities transmission rates were identical to within-
306 community rates (i.e. $w = 1.0$). **(c)** Sample output clusters of Phydelity for a subtree of an example simulation (w
307 $= 0.5$). Tips that were clustered by Phydelity are distinctly coloured according to their cluster membership. By
308 relaxing the monophyletic assumption, Phydelity is capable of detecting paraphyletic clusters (e.g. transmission
309 pair 166-T17 and 171-T17 and cluster subtending 132-T14, 135-T14 and 137-14).
310

311 The phylogenetic trees generated from the simulations had a large number of clusters that
312 were relatively small in size (i.e. percentage of sequences that were part of ground truth
313 clusters with sizes < 8 tips = 33.9% (weight of inter-community transmission rates, w =
314 25%); 55.5% (w = 100%); see Barido-Sottani *et al.* (2018) for more details). Furthermore,
315 these ground truth clusters were not all monophyletic (Figure 2c). As a result, while
316 Phydelity and WPGMA yielded comparable ARI scores (Phydelity: 0.44-0.45 (s.d. = 0.05);
317 WPGMA: 0.44-0.56 (s.d. = 0.05-0.05); Supplementary Table 1), Phydelity's output clusters,
318 which allows paraphyletic clusters (Figure 2c), are substantially purer (mean purity;
319 Phydelity: 0.81-0.88 (s.d. = 0.03); WPGMA: 0.67-0.74 (s.d. = 0.06-0.06)) and have a lower
320 probability of misclassification when compared to WPGMA which assumes clusters are
321 strictly monophyletic (mean I_G; Phydelity: 0.27-0.28 (s.d. = 0.04-0.05); WPGMA: 0.33-0.40
322 (s.d. = 0.04-0.05)). Coverage of sequences clustered by Phydelity lies between 58.2% and
323 61.6%.
324

325 The clustering results from WPGMA presented in this work were based on the optimal
326 distance threshold derived by calibration against the simulated ground-truth. Notably,
327 Phydelity's auto-scaling mitigates the need for threshold calibration and enables application
328 to empirical datasets where ground truth clustering is unavailable, as is typically the case for
329 epidemiological studies.
330

331 *Hepatitis B virus transmission between family members*

332 Phydelity was tested on empirical datasets to demonstrate its applicability on real-world data,
333 including hepatitis B viruses (HBV) collected from residents in the Binh Thuan Province of
334 Vietnam (Matsuo et al. 2017). In such highly endemic regions, HBV is commonly

335 transmitted either vertically from mothers to children during the perinatal period or
336 horizontally between cohabitants of the same household (Matsuo et al. 2017). As complete
337 genome nucleotide sequences were not available for all individuals, a phylogenetic tree was
338 reconstructed using the viral polymerase sequences collected from 41 patients, of which 12 of
339 them were confirmed to be members of three families (i.e. denoted as F2, F3 and F4) by a
340 family survey as well as mitochondrial analyses. Besides Phydelity, the resulting phylogeny
341 was also implemented in ClusterPicker and PhyloPart.
342
343 Phydelity identified three likely transmission clusters that distinguish between the separate
344 family households (Figure 3). At their respective optimal distance thresholds by mean
345 Silhouette index (see Methods), ClusterPicker and PhyloPart achieved similar clustering
346 results. Importantly, Phydelity was able to obtain the same optimal clustering results without
347 optimisation and implementation of a hard-to-interpret distance parameter.
348

a

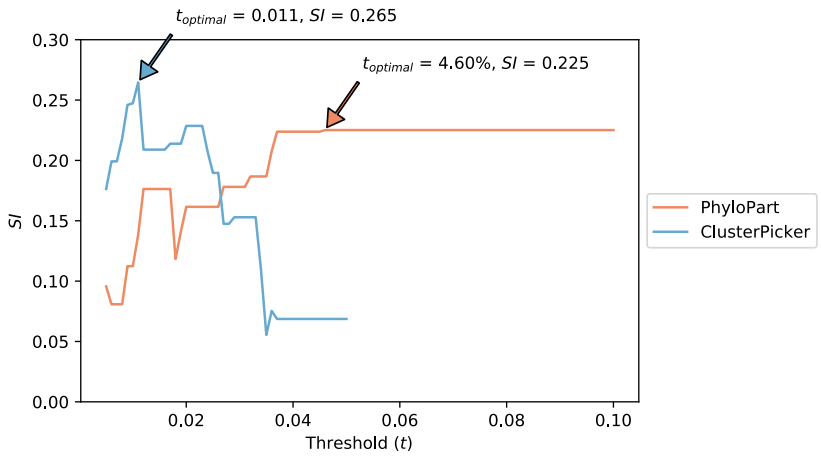

b

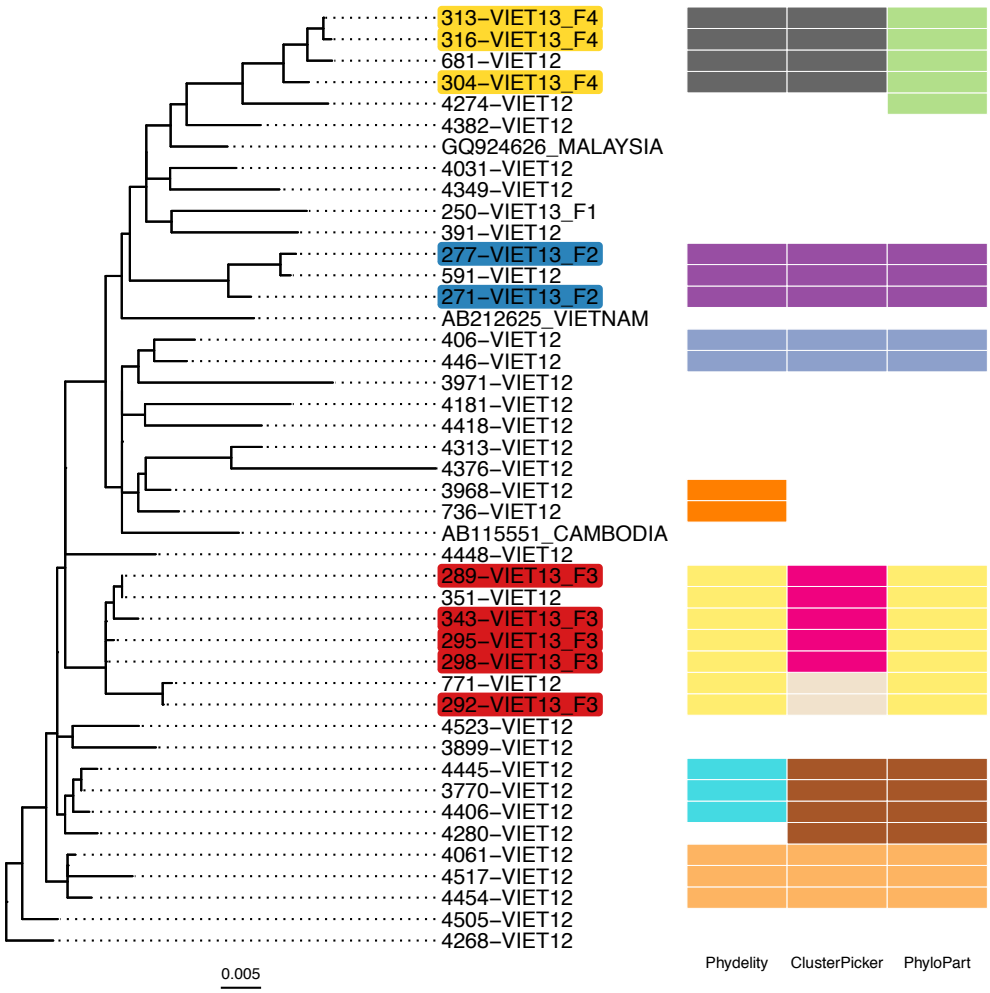

Figure 3. Clustering results of hepatitis B viruses (HBV) collected from residents in the Binh Thuan Province of Vietnam. (**a**) Plots of mean Silhouette index (*SI*) computed for the range of genetic distance thresholds implemented in ClusterPicker and PhyloPart. Clustering results from the lowest optimal distance threshold ($t_{optimal}$) with the highest *SI* value for each method were compared to Phydelity as depicted in **b** (ClusterPicker: $t_{optimal}$ = 0.011 nucleotide/site, *SI* = 0.265; PhyloPart: $t_{optimal}$ = 4.60%, *SI* = 0.225). Plot for ClusterPicker is truncated at ~0.05 nucleotide/site as the entire tree collapsed to single cluster after this threshold. (**b**) Maximum likelihood phylogeny of HBV polymerase sequences derived from viruses collected from 41 patients. 12

356 patients were confirmed to be members of three separate family households (F2, F3 and F4; tip names shaded
357 with a distinct colour for each family). Clustering results from Phydelity are depicted as a heatmap alongside
358 outputs from ClusterPicker and PhyloPart based on their respective $t_{optimal}$. Each distinct colour of the heatmap
359 cells denotes a different cluster.
360

361 *Hepatitis C virus transmission among MSM*

362 Incidence of HCV infections among HIV-negative MSM has been relatively limited as
363 compared to their HIV-positive counterparts. However, the recent uptake of pre-exposure
364 prophylaxis (PrEP) among HIV-negative individuals to prevent HIV infection could pose
365 higher risk of sexually transmitted HCV infections (Volk et al. 2015; Charre et al. 2018). In a
366 study on HIV-positive and HIV-negative MSM patients in Lyon, 108 cases of acute HCV
367 infections (80 primary infections; 28 reinfections) were reported between 2014 and 2017
368 among 96 MSM (72 HIV-positive; 24 HIV-negative, of which 16 (67%) of them were on
369 PrEP; Charre et al. 2018). Separate phylogenetic analyses were performed on a subset of 89
370 (68 HIV-positive; 21 HIV-negative) HCV isolates belonging to genotypes 1a and 4d based on
371 their NS5B sequences. Additionally, 25 HCV sequences from HIV-infected MSM collected
372 before 2014 were included along with 60 control HCV sequences derived from HIV-
373 negative, non-MSM patients residing in the same geographical area as controls. All
374 sequences collected from MSM patients were given strain names in the format of
375 "MAH(ID)_accession" while control sequences from non-HIV, non-MSM patients were
376 denoted as "NCH(ID)_accession" (Figure 4). Phydelity as well as ClusterPicker and
377 PhyloPart were applied to the reconstructed phylogenies, with the latter calibrated over a
378 range of distance thresholds. Again, only clustering results based on the lowest distance
379 threshold maximising the mean Silhouette index for ClusterPicker and PhyloPart were
380 compared to Phydelity's output clusters (see Methods).
381

382 Generally, membership of the MSM transmission clusters and pairs identified by Phydelity
383 across both genotypes were strictly limited to sequences derived from MSM patients.
384 Relaxing the monophyletic assumption by dissociating distantly-related tips from putative
385 monophyletic clusters (see Methods) enables Phydelity to identify likely outlying sequences
386 as evidenced by their relatively longer branch lengths from the cluster ensemble (Table 1 and
387 Figure 4; Genotype 1a: cluster C1 – MAH66 and cluster C3 – MAH31, MAH62 and
388 MAH72; Genotype 4d: cluster C3 – MAH24 and MAH08). In particular, for genotype 1a,
389 even though the mean pairwise distance of MAH72 to members of cluster C3 is within a
390 standard deviation of the latter's within-cluster diversity, its distance to the more distant

391 members (e.g. MAH15 and MAH40, Figure 4) violated the inferred *MPL* (Table 1).
392 Additionally, as a result of distal dissociation, Phydelity distinguishes clusters that are
393 genetically more alike amongst themselves than to those phylogenetically ancestral to it (e.g.
394 cluster C1.1 that is "nested" within cluster C1 for genotype 1a; Figure 4a).
395
396 For both genotypes, Phydelity found multiple clusters that included both HIV-positive and
397 HIV-negative MSM patients (i.e. Genotype 1a: clusters C2 and C3, Figure 4a; Genotype 4d:
398 clusters C2 and C2.2, as well as pair P2, Figure 4b). While it is not clear which of the HIV-
399 negative patients were on PrEP (information not supplied in the original paper), the clustering
400 results from Phydelity were in line with the findings by Charre *et al*. that acute HCV
401 infections among HIV-negative MSM were likely sourced from their HIV-positive
402 counterparts.
403
404 While ClusterPicker managed to consolidate all of the MSM genotype 4d sequences into a
405 single monophyletic cluster (Figure 4b), its clustering of genotype 1a was problematic as a
406 large number of non-MSM control sequences were clustered together with those from MSM
407 patients (Figure 4a). PhyloPart's optimal clustering output was consistent Phydelity's for
408 genotype 1a. However, the larger number of identical sequences in the genotype 4d tree
409 skewed the optimal distance parameter (expressed as *x*-th percentile of the pairwise patristic
410 distribution of the entire phylogeny) to only cluster these identical sequences.
411

Genotype	MPL	Cluster	Mean pairwise patristic distance of cluster (σ)	Outlier	Mean pairwise patristic distance of outliers to cluster members (σ)
1a	0.029	C1	0.011 (0.012)	MAH66	0.043 (0.009)
		C3	0.016 (0.009)	MAH62	0.045 (0.027)
				MAH31	0.041 (0.025)
				MAH72	0.022 (0.015)
4d	0.010	C1	0.006 (0.004)	MAH24	0.019 (0.006)
				MAH08	0.009 (0.005)

412 **Table 1**: Comparing the genetic distance between outlying tips and the clusters they coalescence to with the
413 genetic diversity of those clusters.

a.

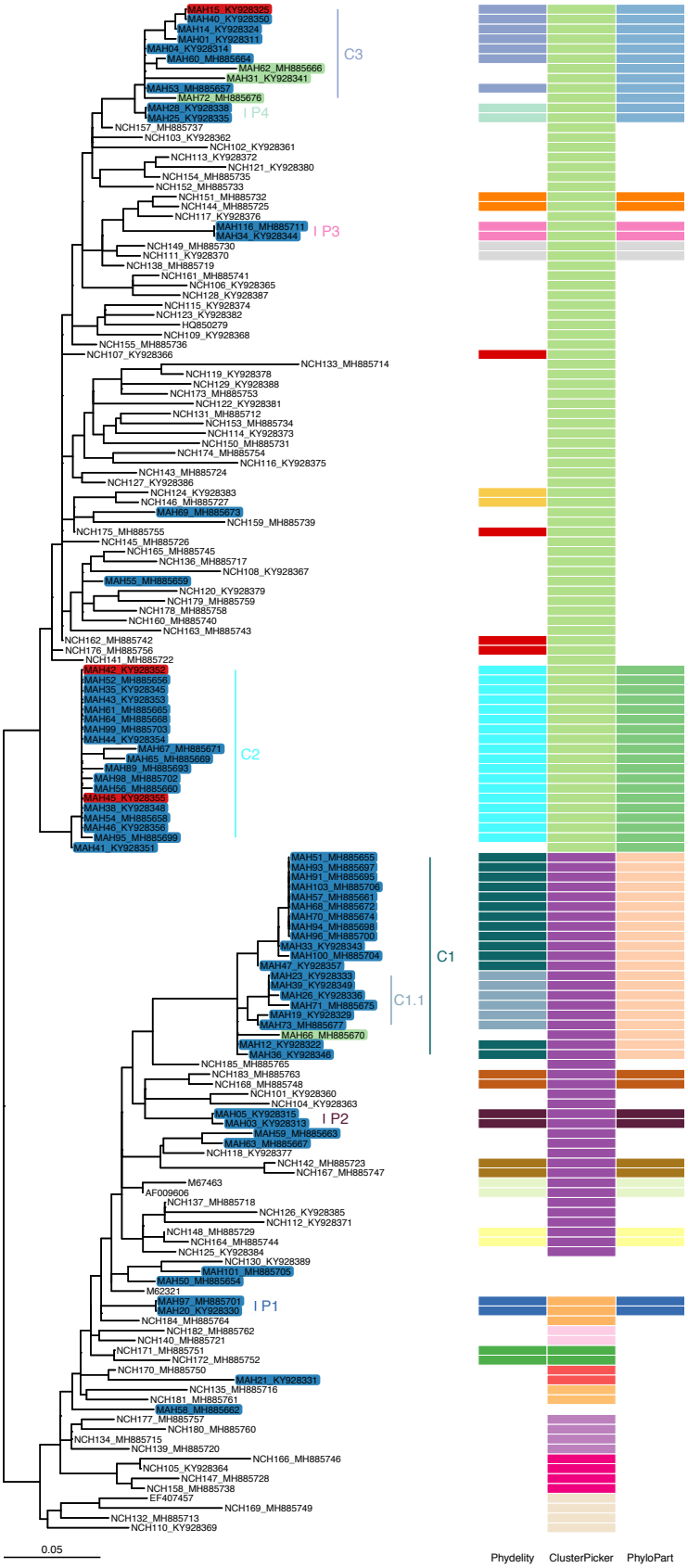
C3
I P4
I P3
C2
C1
C1.1
I P2
I P1
0.05
Phydelity
ClusterPicker
PhyloPart

b.

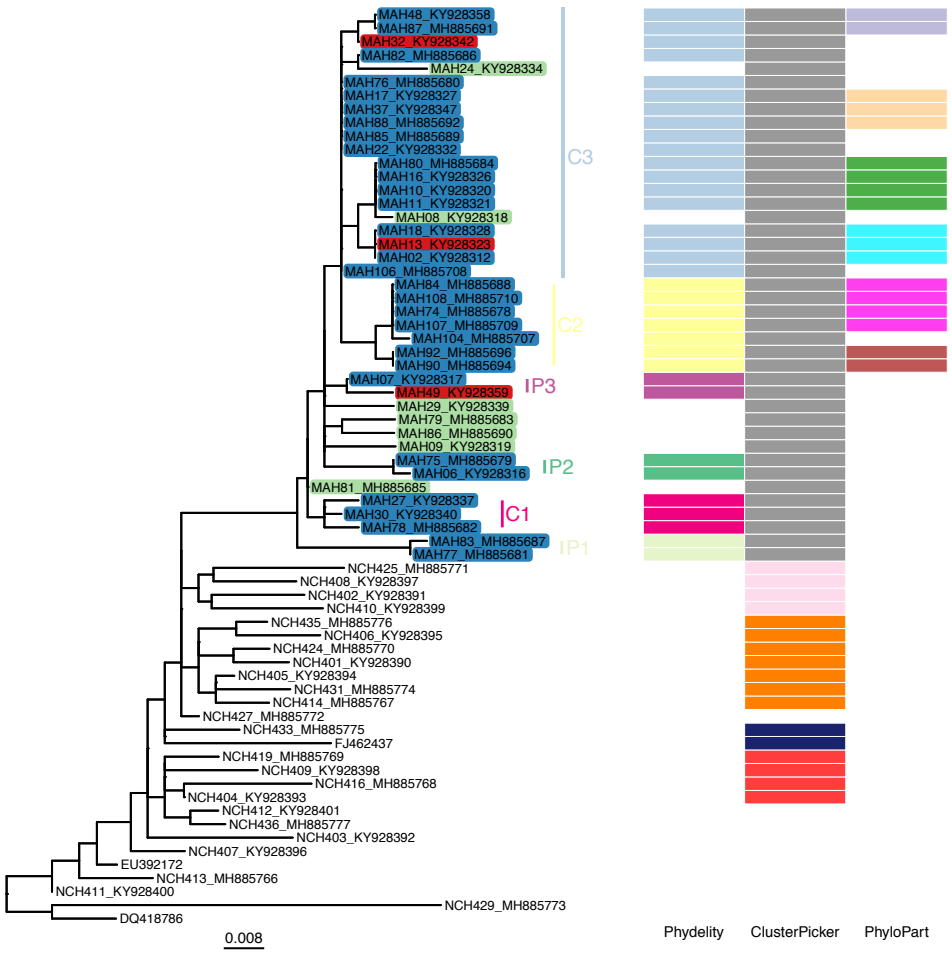

Figure 4. Maximum likelihood phylogeny and clustering results of hepatitis C viruses (HCV) obtained from men who have sex with men (MSM) in Lyon, France. All highlighted tip names denoted in the format "MAH(ID)_accession" were samples from MSM patients (blue: HIV-positive, red: HIV-negative, green: HIV-positive and considered as outlying sequences by Phydelity). Non-highlighted tips were collected from non-HIV, non-MSM patients residing in the same geographic region and time period. Clustering results from Phydelity, ClusterPicker and PhyloPart are depicted as a heatmap. Each distinct colour refers to a different cluster. Similar to the Vietnamese hepatitis B empirical viral datasets (Figure 3a and Supplementary Figure 4), mean Silhouette index was used as the optimality criterion to determine the optimal absolute distance threshold for ClusterPicker and PhyloPart. Only results based on the optimised thresholds are shown here for ClusterPicker and PhyloPart. No parameter optimisation is required for Phydelity. **(a)** Genotype 1a. **(b)** Genotype 4d.

427 *Seasonal A/H3N2 influenza virus infections within a community and the effects of sampling*
428 Phydelity was also applied to A/H3N2 influenza viruses collected from a community-based
429 cohort of 340 households (1431 participants) in Southeastern Michigan, U.S. during the
430 2014/2015 season (McCrone et al. 2018). Of the influenza positive cases, 206 virus samples
431 were collected from 166 individuals that belonged to 81 households and sequenced. As
432 concurrent infections among individuals within the same household do not necessarily imply
433 transmission, McCrone et al. implemented stringent epidemiological as well as genetic
434 distance constraints to identify transmission pairs: (i) the donor and recipient of a
435 transmission pair were of the same household with onset of illness symptoms occurring
436 within 7 days of each other, with the donor having the earlier symptom onset date; (ii) there
437 must be no other potential donors with the same symptom onset date; (iii) symptom onset
438 dates of donor and recipient should not be on the same day unless they were index cases; and
439 (iv) genetic distance between the within-host viral populations of donor and recipient must be
440 below the 5th percentile of the distance distribution of random pairs of infected individuals
441 from the community (McCrone et al. 2018). In total, 50 virus isolates constituting 32 high-
442 quality transmission pairs were identified. Consolidating transmission pairs with overlapping
443 donors and recipients into clusters, there were 22 genetically-validated transmission clusters,
444 comprising of 16 pairs and 6 trios in total.
445
446 Using the phylogeny constructed from the consensus whole genome sequences of all 206
447 viruses, Phydelity was able identify 20 of the 22 high-quality transmission clusters as distinct
448 clusters (Supplementary Figure 5). Applying the same metrics used to assess clustering
449 performance of the simulated dataset earlier and using the high-quality transmission cluster
450 labels as ground truth, Phydelity was able to produce highly pure clusters (97.8%), with a low
451 probability of misclassification ($I_G = 0.022$) and good accuracy (ARI = 0.962), even after
452 accounting for the number of predicted clusters (NMI = 0.993; Table 2). As transmission
453 events defined by McCrone et al. were based on highly conservative criteria imposed on deep
454 sequencing datasets, Phydelity, which operates at the consensus sequence level, could also
455 cluster viruses that did not satisfy these constraints but were still linked epidemiologically by
456 their household identities. As such, Phydelity's clustering results were assessed based on the
457 household association of the clustered individuals as well, yielding slightly diminished but
458 nonetheless high quality performance (Purity = 0.894, $I_G = 0.081$, ARI = 0.791, NMI =
459 0.964; Supplementary Figure 5 and Table 2).

Basis	n_{sample}	$\%_{trans}$	*Purity*	I_G	*ARI*	*NMI*
High-quality transmission clusters	**All**		**0.98**	**0.02**	**0.96**	**0.99**
	52	25%	0.87	0.06	0.72	0.93
		45%	0.87	0.04	0.74	0.95
		70%	0.85	0.07	0.76	0.94
	93	25%	0.94	0.03	0.88	0.98
		45%	0.94	0.03	0.90	0.98
Household	**All**		**0.89**	**0.08**	**0.79**	**0.96**
	52	25%	0.56	0.29	0.35	0.82
		45%	0.73	0.16	0.56	0.90
		70%	0.82	0.11	0.74	0.93
	93	25%	0.75	0.16	0.64	0.92
		45%	0.87	0.11	0.80	0.95

Table 2: Clustering performance of Phydelity on seasonal A/H3N2 influenza viruses collected by McCrone et al. (2018). Ground truth used for clustering assessment is either based on the identities of genetically-validated, high-quality transmission clusters as defined by McCrone et al. or by the patients' households. Besides analysing all of the viruses collected (bolded results), Phydelity was also applied to downsampled datasets consisting of different sample size (n_{sample}) and proportion of sequences derived from the aforementioned high-quality transmission pairs ($\%_{trans}$). Adjusted rand index (*ARI*) measures how accurate the output clusters corresponded with the ground truth labels. *Purity* gives the average extent clusters contain only a single class. Modified Gini index (I_G) is the probbility that a randomly selected sequence would be incorrectly clustered. Normalised mutual information (*NMI*) accounts for the trade-off between clustering quality and number of clusters.

The full A/H3N2 sequence dataset was then randomly sampled to smaller pools of 52 (25%) as well as 93 (45%) isolates to assess how low sampling rates might affect Phydelity's performance. To ensure that sequences involved in high-quality transmission pairs were also sampled, such isolates would constitute different proportions (either 25% or 45%; as well as 70% for pools of 52 sequences only) of the downsampled datasets. 10 distinct downsamples were generated for each sample size/high-quality transmission sequence combination and the average results were tabulated (Table 2).

As the *MPL* is informed by the phylogenetic tree, clustering results will consequently be sensitive to the diversity of closely-related tips within the input phylogeny. Specifically, the closely-related sequences that constitute the *k*-th core patristic distance distribution ($\mathcal{D}_k$) must be homogenous (i.e. similar difference between consecutive distances when $\mathcal{D}_k$ is sorted; see Methods) but sufficiently distinct from the background diversity of the phylogeny. This was demonstrated by the improved clustering results with respect to household identities with

486 greater proportional inclusion of genetically similar, high-quality transmission pairs in the
487 downsampled dataset (Table 2). Furthermore, erroneous clustering of distantly-related tips
488 can be obtained if $\mathcal{D}_k$ has a similar distance distribution relative to the entire tree due to
489 insufficient divergence information from reduced sampling. This is evident from the general
490 decrease in the clustering performance of all downsampled data. In particular, clustering
491 closely-related, high-quality transmission clusters was worse off with a lower sample size.
492
493 *Computational performance*
494 For computational performance, Phydelity can process a phylogeny of 1000 tips, on an
495 Ubuntu 16.04 LTS operating system with an Intel Core i7-4790 3.60 GHz CPU, in ~3
496 minutes using a single CPU core and 253 MB of peak memory usage.
497
498 **Discussion**
499 Phydelity is a statistically-principled tool capable of identifying putative transmission clusters
500 from pathogen phylogenies without the need to introduce arbitrary distance thresholds.
501 Instead, Phydelity infers the maximal patristic distance limit (*MPL*) for cluster designation
502 using the pairwise patristic distance distribution of closely-related tips in the input
503 phylogenetic tree. Unlike other cutpoint-based methods, Phydelity does not assume clusters
504 are strictly monophyletic and can identify paraphyletic clustering owing to its distal
505 dissociation approach. For datasets that span extended periods of time, multiple introductions
506 within the same contact network and concurrent onward transmissions to other communities
507 can result in "nested" introduction events that would go undetected by monophyletic
508 clustering (Barido-Sottani et al. 2018). By relaxing this assumption, not only can Phydelity
509 pick up these "nested" events, it tends to produce clusters that are purer with a lower chance
510 of misclassification while excluding putative outlying tips that are exceedingly distant from
511 the inferred cluster.
512
513 Even though there are algorithmic similarities between PhyCLIP (Han et al. 2019) and
514 Phydelity, clustering results generated by PhyCLIP should not be interpreted as sequences
515 linked by transmission events. For instance, when applied to the HCV genotype 1a NS5B
516 dataset, PhyCLIP clustered 131 of the 155 input sequences into seven clades, all of which
517 encompasses genetically similar viruses of both MSM and non-MSM origins that were
518 endemic in Lyon during a specific period in time. In contrast, Phydelity assigned 73

519 sequences into 12 transmission pairs and 5 transmission clusters that distinguished the
520 underlying MSM transmission events from non-MSM ones (Supplementary Figure 1). A
521 detailed comparison between Phydelity and PhyCLIP can be found in Supplementary
522 Materials.
523
524 One of the key assumptions made by Phydelity is that the transmitted pathogens coalesce to
525 the same most recent common ancestor (MRCA) and that the pairwise genetic distance of
526 internal nodes found between the MRCA and the tips of the cluster to be bounded below
527 *MPL*. While Phydelity does not explicitly equate the inferred phylogeny to a transmission
528 tree, imposing a distance threshold between the internal nodes within a phylogenetic cluster
529 may be construed as an implicit assumption that the internal nodes are representative of
530 transmission events. There are important differences in the interpretation of phylogenetic and
531 transmission trees. The former depicts the shared ancestry between the sampled tips while the
532 latter represents the true transmission history between the transmitted pathogens (Pybus and
533 Rambaut 2009; Ypma et al. 2013). It should be noted that Phydelity neither attributes any
534 interpretation of transmission events to the internal nodes nor does it relate branch lengths of
535 the phylogenetic tree, which correlate with the timing of coalescence, to transmission times.
536 Restricting the distances between internal nodes below the *MPL* is strictly meant to increase
537 conservatism in identifying clusters that are as closely-related as possible.
538
539 There have also been criticisms that non-parametric cluster identification by genetic
540 similarity is biased towards the detection of recent infections as opposed to discerning
541 variations in transmission rates between different subpopulations, which can be further
542 exacerbated by oversampling (Poon 2016; Dearlove et al. 2017; Le Vu et al. 2018). While
543 this caveat limits the interpretation of the inferred transmission clusters, it does not render all
544 phylogenetic clustering tools obsolete. Phylogenetic clustering tools supplemented by
545 epidemiological meta-data can still be used to systematically identify infection trends,
546 potential risk factors and target subpopulations, as demonstrated by multiple epidemiological
547 studies of different measurably-evolving pathogens (Matsuo et al. 2017; de Oliveira et al.
548 2017; Charre et al. 2018).
549
550 Additionally, constructing a phylogenetic tree can be a computational bottleneck for large
551 sequence datasets. As an alternative, genetic distance-based clustering algorithms such as

HIV-TRACE (Kosakovsky Pond et al. 2018) which negate the need to build a phylogenetic tree have becoming increasingly popular. However, HIV-TRACE still requires users to specify an arbitrary absolute distance threshold. Additionally, while it performed better than other existing phylogenetic clustering methods, HIV-TRACE did not preclude problems with bias towards higher sampling rates (Poon 2016).

Despite its limitations, clustering results generated by Phydelity for the simulation and empirical datasets in this study demonstrate its superior performance over current widely used phylogenetic clustering methods. Importantly, Phydelity obviates the need for users to define or optimise non-biologically-informed distance thresholds. Phydelity is fast, generalisable, and freely available at https://github.com/alvinxhan/Phydelity.

Acknowledgements

We would like to thank Frits Scholer for his assistance with optimising Phydelity, as well as Jelle Koopsen and Velislava Petrova for their intellectual contributions.

Data availability

Phydelity is freely available on https://github.com/alvinxhan/Phydelity. All simulated datasets were downloaded from Villandre et al. (2016). Genbank accession numbers of HBV polymerase sequences: AB212625, GQ924626, AB115551, LC57377-LC57378, LC60789-LC60790, LC63767, LC64366-LC64378, LC64380-LC64381, LC80779-LC80783, LC80785, LC80787-LC80800, and LC80802-LC80804. Genbank accession numbers of HCV NS5B sequences: AF9606, EF407457, HQ850279, EU392172, FJ462437, DQ418786, M62321, MH885654-MH885777, and KY928311-KY928401. The A/H3N2 influenza virus consensus sequences were downloaded from https://github.com/lauringlab/Host_level_IAV_evolution. Jupyter notebooks used to analyse both simulated and empirical datasets can be downloaded from https://github.com/alvinxhan/Phydelity/tree/master/manuscript.

Funding

A.X.H. was supported by the A*STAR Graduate Scholarship programme from A*STAR to carry out his PhD work via collaboration between Bioinformatics Institute (A*STAR) and NUS Graduate School for Integrative Sciences and Engineering from the National University

585 of Singapore. E.P. was funded by the Gates Cambridge Trust (Grant number: OPP1144).
586 S.M.S. was supported by the A*STAR HEIDI programme (Grant number: H1699f0013) and
587 Bioinformatics Institute (A*STAR).
588

589 **References**

590 Aldous JL, Pond SK, Poon A, Jain S, Qin H, Kahn JS, Kitahata M, Rodriguez B, Dennis AM,
591 Boswell SL, et al. 2012. Characterizing HIV Transmission Networks Across the United
592 States. Clin. Infect. Dis. 55(8):1135–1143.

593 Ambrosioni J, Junier T, Delhumeau C, Calmy A, Hirschel B, Zdobnov E, Kaiser L, Yerly S,
594 Study the SHIVC. 2012. Impact of highly active antiretroviral therapy on the molecular
595 epidemiology of newly diagnosed HIV infections. AIDS 26(16):2079–2086.

596 Barido-Sottani J, Vaughan TG, Stadler T. 2018. Detection of HIV transmission clusters from
597 phylogenetic trees using a multi-state birth–death model. J. R. Soc. Interface 15(146).

598 Bartlett SR, Jacka B, Bull RA, Luciani F, Matthews G V., Lamoury FMJ, Hellard ME,
599 Hajarizadeh B, Teutsch S, White B, et al. 2016. HIV infection and hepatitis C virus genotype
600 1a are associated with phylogenetic clustering among people with recently acquired hepatitis
601 C virus infection. Infect. Genet. Evol. 37:252–258.

602 Bezemer D, Cori A, Ratmann O, van Sighem A, Hermanides HS, Dutilh BE, Gras L,
603 Rodrigues Faria N, van den Hengel R, Duits AJ, et al. 2015. Dispersion of the HIV-1
604 Epidemic in Men Who Have Sex with Men in the Netherlands: A Combined Mathematical
605 Model and Phylogenetic Analysis. PLOS Med. 12(11):e1001898.

606 Breiman L, Friedman J, Stone CJ, Olshen RA. 1984. Classification and regression trees.
607 Florida.

608 Brenner BG, Roger M, Routy J-P, Moisi D, Ntemgwa M, Matte C, Baril J-G, Thomas R,
609 Rouleau D, Bruneau J, et al. 2007. High Rates of Forward Transmission Events after
610 Acute/Early HIV-1 Infection. J. Infect. Dis. 195(7):951–959.

611 Campbell F, Strang C, Ferguson N, Cori A, Jombart T. 2018. When are pathogen genome
612 sequences informative of transmission events? PLOS Pathog. 14(2):e1006885.

613 Charre C, Cotte L, Kramer R, Miailhes P, Godinot M, Koffi J, Scholtès C, Ramière C. 2018.
614 Hepatitis C virus spread from HIV-positive to HIV-negative men who have sex with men.
615 PLoS One 13(1):e0190340.

616 Coll F, Harrison EM, Toleman MS, Reuter S, Raven KE, Blane B, Palmer B, Kappeler ARM,
617 Brown NM, Török ME, et al. 2017. Longitudinal genomic surveillance of MRSA in the UK
618 reveals transmission patterns in hospitals and the community. Sci. Transl. Med.
619 9(413):eaak9745.

620 Dearlove BL, Xiang F, Frost SDW. 2017. Biased phylodynamic inferences from analysing
621 clusters of viral sequences. Virus Evol. 3(2):vex020.

622 Gardy JL, Loman NJ. 2017. Towards a genomics-informed, real-time, global pathogen
623 surveillance system. Nat. Rev. Genet. 19(1):9–20.

624 Grabowski MK, Redd AD. 2014. Molecular tools for studying HIV transmission in sexual
625 networks. Curr. Opin. HIV AIDS 9(2):126–133.

626 Han AX, Parker E, Scholer F, Maurer-Stroh S, Russell CA. 2019. Phylogenetic Clustering by
627 Linear Integer Programming (PhyCLIP). Mol. Biol. Evol. 36(7):1580–1595.

628 Hubert L, Arabie P. 1985. Comparing partitions. J. Classif. 2(1):193–218.

629 Jacka B, Applegate T, Krajden M, Olmstead A, Harrigan PR, Marshall BDL, DeBeck K,
630 Milloy M-J, Lamoury F, Pybus OG, et al. 2014. Phylogenetic clustering of hepatitis C virus
631 among people who inject drugs in Vancouver, Canada. Hepatology 60(5):1571–1580.

632 Kosakovsky Pond SL, Weaver S, Leigh Brown AJ, Wertheim JO. 2018. HIV-TRACE
633 (TRAnsmission Cluster Engine): A tool for large scale molecular epidemiology of HIV-1 and
634 other rapidly evolving pathogens. Mol. Biol. Evol. 35(7):1812–1819.

635 Manning CD, Raghavan P, Schütze H. 2008. Introduction to Information Retrieval. New
636 York, NY, USA: Cambridge University Press

637 Matsuo J, Do SH, Yamamoto C, Nagashima S, Chuon C, Katayama K, Takahashi K, Tanaka
638 J. 2017. Clustering infection of hepatitis B virus genotype B4 among residents in Vietnam,
639 and its genomic characters both intra- and extra-family. PLoS One 12(7):e0177248.

640 McCrone JT, Woods RJ, Martin ET, Malosh RE, Monto AS, Lauring AS. 2018. Stochastic
641 processes constrain the within and between host evolution of influenza virus. Elife 7:e35962.

642 de Oliveira T, Kharsany ABM, Gräf T, Cawood C, Khanyile D, Grobler A, Puren A, Madurai
643 S, Baxter C, Karim QA, et al. 2017. Transmission networks and risk of HIV infection in
644 KwaZulu-Natal, South Africa: a community-wide phylogenetic study. Lancet HIV 4(1):e41–
645 e50.

646 Poon AFY. 2016. Impacts and shortcomings of genetic clustering methods for infectious
647 disease outbreaks. Virus Evol. 2(2):vew031.

648 Prosperi MCFF, Ciccozzi M, Fanti I, Saladini F, Pecorari M, Borghi V, Di Giambenedetto S,
649 Bruzzone B, Capetti A, Vivarelli A, et al. 2011. A novel methodology for large-scale
650 phylogeny partition. Nat. Commun. 2:321.

651 Pybus OG, Rambaut A. 2009. Evolutionary analysis of the dynamics of viral infectious
652 disease. Nat. Rev. Genet. 10(8):540–550.

653 Ragonnet-Cronin M, Hodcroft E, Hué S, Fearnhill E, Delpech V, Brown AJL, Lycett S.
654 2013. Automated analysis of phylogenetic clusters. BMC Bioinformatics 14(1):317.

655 Rousseeuw PJ. 1987. Silhouettes: A graphical aid to the interpretation and validation of
656 cluster analysis. J. Comput. Appl. Math. 20:53–65.

657 Rousseeuw PJ, Croux C. 1993. Alternatives to the Median Absolute Deviation. J. Am. Stat.

658 Assoc. 88(424):1273–1283.

659 Stamatakis A. 2014. RAxML version 8: a tool for phylogenetic analysis and post-analysis of
660 large phylogenies. Bioinformatics 30(9):1312–1313.

661 Villandre L, Stephens DA, Labbe A, Günthard HF, Kouyos R, Stadler T, Study TSHIVC.
662 2016. Assessment of Overlap of Phylogenetic Transmission Clusters and Communities in
663 Simple Sexual Contact Networks: Applications to HIV-1. PLoS One 11(2):e0148459.

664 Volk JE, Marcus JL, Phengrasamy T, Hare CB. 2015. Incident Hepatitis C Virus Infections
665 Among Users of HIV Preexposure Prophylaxis in a Clinical Practice Setting. Clin. Infect.
666 Dis. 60(11):1728–1729.

667 Le Vu S, Ratmann O, Delpech V, Brown AE, Gill ON, Tostevin A, Fraser C, Volz EM.
668 2018. Comparison of cluster-based and source-attribution methods for estimating
669 transmission risk using large HIV sequence databases. Epidemics 23:1–10.

670 Ypma RJF, van Ballegooijen WM, Wallinga J. 2013. Relating phylogenetic trees to
671 transmission trees of infectious disease outbreaks. Genetics 195(3):1055–1062.

672